CHINESE JOURNAL OF PHYSICS VOL. 40, NO. 1 FEBRUARY 2002

The Order Parameters of a Transverse Ferromagnetic Superlattice with Antiferromagnetic Interface Coupling

M. Bentaleb, B. Laaboudi, and N. El Aouad
Département de Physique, Faculté des Sciences,
Université Moulay Ismail, B.P. 4010,
Meknès, Morocco

(Received October 12, 2001)

We have studied the magnetic properties of a ferroelectric superlattice consisting of two ferromagnetics, with L_a layers of spins S_a and L_b layers of spins S_b with antiferromagnetic interface coupling. The two sublattice magnetizations and a total magnetization are calculated for different sets of interaction parameters and transverse field over the whole range of temperatures. We have obtained some interesting results such as the compensation temperature which is found when $S_a \neq S_b$ within a certain range of exchange interactions and decreases when the transverse field increases.

PACS. 05.50.+q – Lattice theory and statistics; Ising problems.

I. Introduction

Extensive investigations have been made on magnetic superlattices during the past years. Experimentally, magnetic superlattices Dy/Y [1] and superlattices of rare-earth (RE) and transition metal (TM) [2-5] have been obtained by advanced techniques. The RE/TM superlattices show an interesting magnetic coupling behavior. The interlayer coupling is considered to be ferromagnetic for light REs, while it is antiferromagnetic for heavy REs. Theoretically, various Heisenberg models and the Green function technique are usually used to study the magnetic properties of the superlattices. Akjouj *et al.* [6] have studied bulk and surface magnons in a ferromagnetic film sandwiched betweeen two different semi-infinite ferromagnets. Zhou and Lin [7] have investigated magnetic excitations of a Heisenberg ferromagnetic superlattice consisting of alternative layers of A and B atoms. In [11-13], the authors have investigated multilayers consisting of different ferromagnetic materials with antiferromagnetic coupling at the interfaces and obtained some interesting results.

Theoretically, phase transitions and soft modes in ferroelectric superlattices were studied by Schwenk *et al.* [11-12], using the Ginzburg-Landau phenomenological theory based on the Ising model in a transverse field, which were originally introduced by De Gennes [13] .Despite the simplicity of the transverse Ising model, it is successful in describing the phase transition behavior of ferroelectrics [14]. By modifying the exchange coupling and the transverse field at the surface, Wang *et al.* [15, 16] and Saber *et al.* [17] successfully extended the transverse Ising model to the study of surface and size effects in ferroelectrics; the critical temperature as well as the phase diagrams as functions of surface parameters and film thickness were investigated [15-17]. The transverse Ising model has also been applied to many other systems, such as the semi-infinite systems of a localized surface spin wave [18] and surface magnetism [19]. In most of the discussions [15-19], only the nearest-neighbor interactions were considered and this simplification seems reasonable in ferromagnets where short-range interactions dominate.

In our previous studies on ferromagnetic superlattices, some interesting results have been obtained [20-24].

In this paper, we shall study a transverse magnetic Ising superlattice of two ferro-magnetic materials with L_a layers of spins S_a, and L_b layers of spins $S_b (L_a = L_b = 2)$ with antiferro-magnetic interface coupling. We use effective field theory, as it is belived to be far superior to the standard mean-field approximation. In section II, we outline the formalism and derive the equation that the layer magnetizations only for $S_a = 1/2$ and $S_b = 1/2$, the formalism for $S_b = 1$ has been detailed in our previous paper [22]. Numerical results are discussed in section III. A brief conclusion is given in Section IV.

II. Model and formalism

We consider a superlattice consisting of two different ferromagnetic materials A and B stacked alternately. For simplicity, we restrict our attention to the case of a simple chbic structure. The periodic condition suggests that we only have to consider one unit cell. The situation is shown in Fig. 1. The ferromagnetic exchange coupling between the nearest-neighbor spins in A (B) is denoted by $J_a (J_b)$, while the transverse field is expressed by - . Here, we consider the interface to be composed of two layers (L_a and $L_a + 1$). J_{ab} stands for the antiferromagnetic exchange coupling between the nearest-neighbor spins across the interface ($J_{ab} < 0$). The number of atomic layers in material A (B) is L_a (L_b) and the thickness of the cell is $L = L_a + L_b$. The Hamiltonian of this system is given by

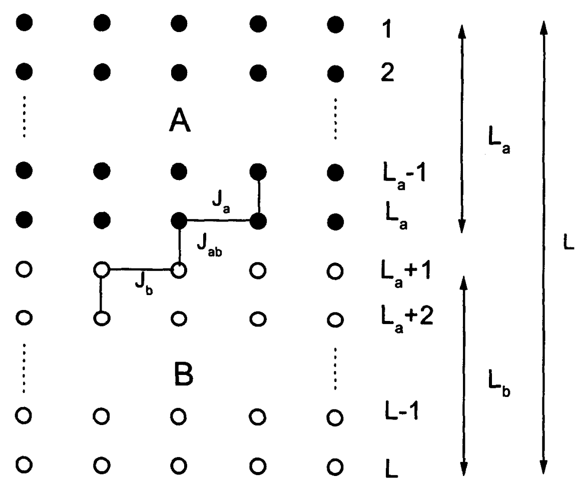

FIG. 1. Sketch of a unit cell of the superlattice.

$$H = -\sum_{(i,j)} J_{ij}\sigma_i^z\sigma_j^z - \Omega\sum_i \sigma_i^x, \tag{1}$$

where the first sum runs over all nearest-neighbor pairs, the second sum is taken over the spins, and J_{ij} stands for one of the three coupling constants (J_a, J_b, J_{ab}), depending on the location of the spin pairs ($J_a > 0$, $J_b > 0$ and $J_{ab} < 0$). Using effective field theory [23, 24], the layer longitudinal magnetizations are given by:

$$\begin{aligned}\sigma_{1,z} = {} & \frac{1}{2^{N+2N_0}}\sum_{i_1=0}^{N}\sum_{i_2=0}^{N_0}\sum_{i_3=0}^{N_0} C_{i_1}^{N}C_{i_2}^{N_0}C_{i_3}^{N_0}(1-2\sigma_{1,z})^{i_1}(1+2\sigma_{1,z})^{N-i_1}(1-2\sigma_{L,z})^{i_2}\\ & (1+2\sigma_{L,z})^{N_0-i_2}(1-2\sigma_{2,z})^{N_0-i_3}\\ & F\left[\frac{1}{2}((N-2i_1)+R_2(N_0-2i_2)+(N_0-2i_3)),\beta\right],\end{aligned} \tag{2}$$

$$\begin{aligned}\sigma_{n,z} = {} & \frac{1}{2^{N+2N_0}}\sum_{i_1=0}^{N}\sum_{i_2=0}^{N_0}\sum_{i_3=0}^{N_0} C_{i_1}^{N}C_{i_2}^{N_0}C_{i_3}^{N_0}(1-2\sigma_{n,z})^{i_1}(1+2\sigma_{n,z})^{N-i_1}\\ & (1-2\sigma_{n-1,z})^{i_2}(1+2\sigma_{n-1,z})^{N_0-i_2}(1-2\sigma_{n+1,z})^{i_3}(1+2\sigma_{n+1,z})^{N_0-i_3}\\ & F\left[\frac{1}{2}((N-2i_1)+(N_0+2i_2)+(N_0-2i_3)),\beta\right],\\ & \text{for } 2\le n\le l_a-1\end{aligned} \tag{3}$$

$$\begin{aligned}\sigma_{L_a,z} = {} & \frac{1}{2^{N+2N_0}}\sum_{i_1=0}^{N}\sum_{i_2=0}^{N_0}\sum_{i_3=0}^{N_0} C_{i_1}^{N}C_{i_2}^{N_0}C_{i_3}^{N_0}(1-2\sigma_{L_a,z})^{i_1}(1+2\sigma_{L_a,1})^{N-i_1}\\ & (1-2\sigma_{L_a+1,z})^{i_2}(1+2\sigma_{L_a+1,z})^{N_0-i_2}(1-2\sigma_{L_a-1,z})^{i_3}(1+2\sigma_{L_a-1,z})^{N_0-i_3}\\ & F\left[\frac{1}{2}((N-2i_1)+R_2(N_0-2i_2)+(N_0-2i_3)),\beta\right],\end{aligned} \tag{4}$$

$$\begin{aligned}\sigma_{L_{a+1},z} = {} & \frac{1}{2^{N+2N_0}}\sum_{i_1=0}^{N}\sum_{i_2=0}^{N_0}\sum_{i_3=0}^{N_0} C_{i_1}^{N}C_{i_2}^{N_0}C_{i_3}^{N_0}(1-2\sigma_{L_{a+1},z})^{i_1}(1+2\sigma_{L_{a+1},1})^{N-i_1}\\ & (1-2\sigma_{L_a,z})^{i_2}(1+2\sigma_{L_a,z})^{N_0-i_2}(1-2\sigma_{L_{a+2},z})^{i_3}(1+2\sigma_{L_{a+2},z})^{N_0-i_3}\\ & F\left[\frac{1}{2}(R_1(N-2i_1)+R_2(N_0-2i_2)+R_1(N_0-2i_3)),\beta\right],\end{aligned} \tag{5}$$

$$\begin{aligned}\sigma_{p,z} = {} & \frac{1}{2^{N+2N_0}}\sum_{i_1=0}^{N}\sum_{i_2=0}^{N_0}\sum_{i_3=0}^{N_0} C_{i_1}^{N}C_{i_2}^{N_0}C_{i_3}^{N_0}(1-2\sigma_{p,z})^{i_1}(1+2\sigma_{p,z})^{N-i_1}\\ & (1+2\sigma_{p-1,z})^{N_0-i_2}(1-2\sigma_{p+1,z})^{i_3}(1+2\sigma_{p+1,z})^{N_0-i_3}\\ & F\left[\frac{1}{2}R_1((N-2i_1)+(N_0-2i_2)+(N_0-2i_3)),\beta\right],\\ & \text{for } L_a+2\le p\le L-1\end{aligned} \tag{6}$$

$$\sigma_{L,z} = \frac{1}{2^{N+2N_0}} \sum_{i_1=0}^{N} \sum_{i_2=0}^{N_0} \sum_{i_3=0}^{N_0} C^{N}_{i_1} C^{N_0}_{i_2} C^{N_0}_{i_3} (1-2\sigma_{L,z})^{i_1}(1+2\sigma_{L,z})^{N-i_1}$$
$$(1-2\sigma_{1,z})^{i_2}(1+2\sigma_{1,z})^{N_0-i_2}(1-2\sigma_{L-1,z})^{i_3}(1+2\sigma_{L-1,z})^{N_0-i_3}$$
$$F\left[\frac{1}{2}(R_1(N-2i_1)+R_2(N_0-2i_2)+R_1(N_0-2i_3)),\Omega\right]; \quad (7)$$

where

$$F(y;\Omega) = \frac{1}{2}\frac{y}{(y^2+\Omega^2)^{1/2}}\tanh\left[\frac{1}{2}(y^2+\Omega^2)^{1/2}\right] \quad (8)$$

and N and N_0 are the numbers of nearest neighbors in the plane and between adjacent planes, respectively ($N = 4$ and $N_0 = 1$ in the case of a simple cubic lattice), $C^l_K = \frac{l!}{k!(l-k)!}$, $R_1 = \frac{J_b}{J_a}$ and $R_2 = \frac{J_{ab}}{J_a}$. The periodic condition of the superlattice has to be satisfied, namely, $\sigma_{0,z} = \sigma_{L,z}$ and $\sigma_{L+1,z} = \sigma_{1,z}$.

We have then obtained the self consistent equations for the magnetizations (equations 2-7) that can be solved directly by numerical iteration. No further algebraic manipulation is necessary. This is the advantage of introducing the probability distribution technique. The same equations hold for any arbitrary structure and, therfore, results for different structures can be obtained without carrying out the detailed algebra encountered when employing other techniques.

In order to investigate the behavior of the compensation temperature (at which the total magnetization m is zero since the two sublattice magnetizations m_a and m_b cancel out), we calculate the total magnetization which is defined as

$$m = \frac{1}{2}(m_a + m_b); \quad (9)$$

where

$$m_a = \frac{\sigma_{1,z} + \sigma_{2,z} \ldots + \sigma_{a,z}}{L_a} \quad (10)$$

and

$$m_b = \frac{\sigma_{L_a+1,z} + \sigma_{L_a+2,z} \ldots + \sigma_{L,z}}{L_b}. \quad (11)$$

III. Results and discussion

III-1. Calculation of the longitudinal magnetization at zero magnetic field:

Fig. 2 shows the thermal variations of the sublattice magnetizations m_a (solid curves) and m_b (dashed curves) for $S_a = S_b = 1/2$, $R_1 = 0.01$ and $R_2 = -0.3$. The curves are the same when we change the antiferromagnetic interface exchange interaction.

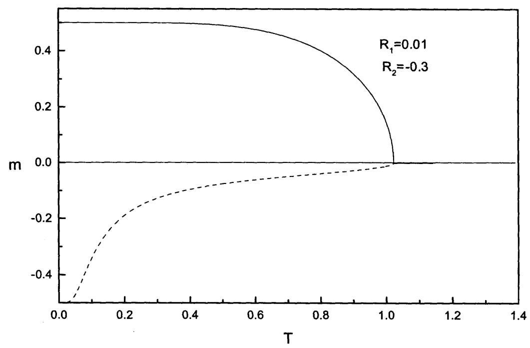

FIG. 2. The temperature dependence of the sublattice longitudinal magnetizations m_a (solid curve) and m_b (dashed curve), for R_1 = J_b=J_a = 0:01, R_2 = J_{ab}=J_a = ¡ 0:3, - = 0 and S_a = S_b = 1=2.

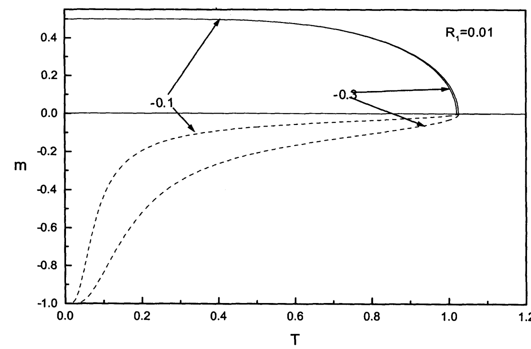

FIG. 3. The temperature dependence of the sublattice longitudinal magnetizations m_a (solid curve) and m_b (dashed curve), for R_1 = J_b=J_a = 0:01, - = 0, S_a = 1=2 and S_b = 1. The number accompanying each curve is the value of R_2.

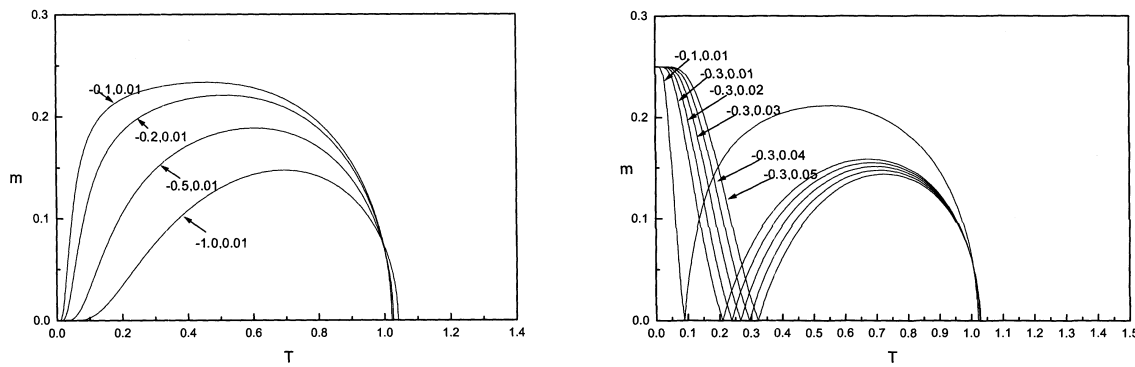

(a) (b)

FIG. 4. (a) The temperature dependence of the total longitudinal magnetization of the superlattice for - = 0 and S_a = S_b = 1=2. The two numbers accompanying each curve are the values of R_2 and R_1 respectively. (b) The temperature dependence of the total longitudinal magnetization of the superlattice for - = 0, S_a = 1=2 and S_b = 1. The two numbers accompanying each curve are the values of R_2 and R_1 respectively.

In Fig. 3, the solid curves and the dashed curves correspond, respectively, to the sublattice magnetizations m_a and m_b for S_a = 1=2, S_b = 1 and R_1 = 0.01. The number accompanying each curve corresponds to R_2. We can see from these two figures that the magnetization m_a of the sublattice A decreases monotonically from 0.5 and reaches zero at the critical temperature T_c. In the sublattice B, even when S_b = 1, the magnetization increases rapidly from its minimum value (¡ 0.5 for S_b = 1=2 and ¡ 1 for S_b = 1) but slowly approaches zero at the critical temperature T_c. For the sublattice (1/2, 1/2) (Fig. 2), the magnetization of each sublattice doesn't depend on the antiferromagnetic interface exchange, although we have the contray situation for the superlattice (1/2, 1) (see Fig. 3).

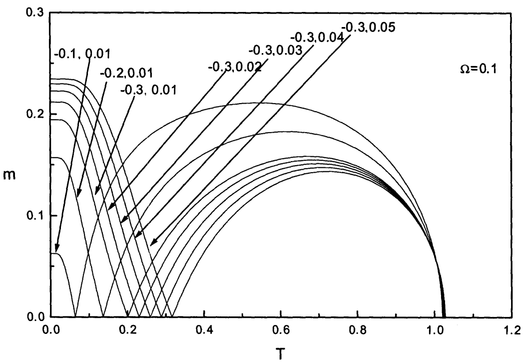

FIG. 5. The temperature dependence of the total longitudinal magnetization of the superlattice for $\Omega = 0.1$, $S_a = 1/2$ and $S_b = 1$. The two numbers accompanying each curve are the values of R_2 and R_1 respectively.

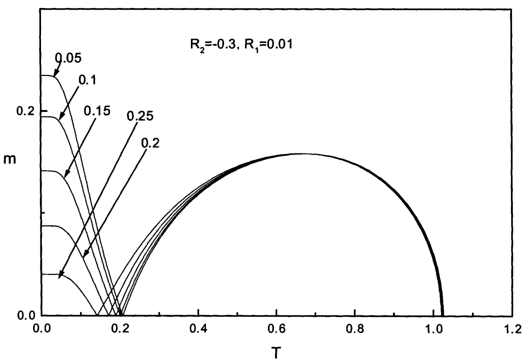

FIG. 6. The temperature dependence of the total longitudinal magnetization of the superlattice for $R_1 = J_b/J_a = 0.01$, $R_2 = J_{ab}/J_a = -0.3$, $S_a = 1/2$ and $S_b = 1$. The number accompanying each curve is the value of the transverse field Ω.

Figures 4a and 4b show the temperature dependence of the total magnetization m, for $S_a = S_b = 1/2$ and for $S_a = 1/2$ and $S_b = 1$, respectively. The two numbers accompanying each curve correspond to R_2 and R_1 respectively. We can see from these two figures that the compensation temperature exists only when $S_a \neq S_b$. The compensation temperature decreases when R_1 or $|R_2|$ decreases. This result can be used to explain the experimental facts of a Co/Tb superlattice [4]. In a Co/Tb superlattice, with the increase of the layer thickness, the effective coupling R_1 in the Tb layer and the effective coupling $|R_2|$ between the Co and Tb layers decrease, thus the compensation temperature decreases.

III-2. The effect of the transverse field on the longitudinal magnetizations: $S_a = 1/2$ and $S_b = 1$

To investigate the effect of the transverse field on the compensation temperature, we have studied the dependance of the total longitudinal magnetization for different values of R_1 and R_2 and for $\Omega = 0.1$ (see Fig. 5). The two numbers accompanying each curve correpond to R_2 and R_1, respectively. We can have the same conclusions that we have from Fig. 3b (for $\Omega = 0$). In addition, we can see that the maximum of the magnetization and the compensation temperature decrease when we increase Ω. This last result is well seen in Fig. 6, which shows clearly that the compensation temperature decreases when the transverse field increases.

IV. Conclusion

In conclusion, the effect of the transverse field on the magnetizations of a ferromgnetic superlattice with antiferromagnetic interlayer coupling was investigated using the effective field theory with a probability distribution technique that accounts for the single-site spin correlations. The intra and interlayer interactions on sublattice magnetizations are examined at zero transverse field and when the transverse field is homogeneous in the superlattice. The study of the total magnetization shows that the compensation temperature exists only for $S_a \neq S_b$ and decreases when R_1 or $|R_2|$ decreases. This result can be used to explain the experimental facts of a Co/Tb superlattice. The application of the transverse field causes a decrease of the total magnetization and the compensation temperature.

References

[1] R. Du, F. Tsui and C. P. Flynn, Phys. Rev. B **38**, 2941 (1988).
[2] Y. Kamiguchi, Y. Hayakawa and H. Fujimori, Appl. Phys. Lett. **55**, 1918 (1989).
[3] T. Tejada, F. Badia, B. Martinez and J. M. Ruiz, J. Magn. Magn. Mater **101**, 181 (1991).
[4] L. Ertl, G. Endl and H. Hoffman, J. Magn. Magn. Mater **113**, 227 (1992).
[5] M. Sajieddine *et al*., J. Magn. Magn. Mater **113**, 243 (1992).
[6] A. Akjouj, B. Sylla, P. Zielinski and L. Dobrzynski, Phys. Rev. B **37**, 5670 (1988).
[7] Y. F. Zhou and T. H. Lin, Phys. Lett. A **134**, 257 (1989).
[8] R. E. Camley, Phys. Rev. B, **39**, 12316 (1989).
[9] J. G. Lepage and R. E. Camley, Phy. Rev. Lett **65**, 1152 (1990).
[10] A. Moschel and K. D. Usadel, J. Magn. Magn. Mater **136**, 99 (1994).
[11] D. Schwenk, F. Fishman, and F. Schwabl, Ferroelectrics **104**, 349 (1990).
[12] D. Schwenk, F. Fishman and F. Schwabl, J. Phys.: Condens. Matter **2**, 5409 (1990).
[13] P. G. De Gennes, Solid State Commun. **1**, 132 (1963).
[14] R. Blinc and B. Zeks, *Soft Modes in Ferroelectrics and antiferroelectrics*, (Amsterdam 1974).
[15] C. L. Wang, W. L. Zhong and P. L Zhang, J. Phys.: Condens. Matter **3**, 4743 (1992).
[16] H. K. Sy, J. Phys.: Condens, Matter **5**, 1213 (1993).
[17] M. Saber *et al.*, Phys. Rev. B **59**, 6908 (1999).
[18] M. G. Cottam, D. R. Tilley and B. Zeks, J. Phys. C **17**, 1793 (1984).
[19] I. Tamura, E. F. Sarmento and T. Kaneyoshi, J. Phys. C **17**, 3207 (1984).
[20] N. El Aouad, B. Laaboudi, M. Kerouad and M. Saber, Phys. Stat. Sol(b), **221**, 737 (2000).
[21] N. El Aouad, B. Laaboudi, M. Kerouad and M. Saber, Physica Scripta, **63**, 247 (2001).
[22] N. El Aouad *et al.*, Chin. J. Phys. **38**, 863 (2000).
[23] N. El Aouad, B. Laaboudi, M. Kerouad and M. Saber, Phys. Review B, **63**, 167 (2001).
[24] N. El Aouad, B. Laabdudi, M. Kerouad and M. Saber, J. Phys.: Condens. Matter, **13**, 797 (2001).